



This is a repository copy of *Microstructure and durability of alkali-activated materials as key parameters for standardization*.

White Rose Research Online URL for this paper:  
<http://eprints.whiterose.ac.uk/86434/>

Version: Accepted Version

---

**Article:**

van Deventer, J.S.J., San Nicolas, R., Ismail, I. et al. (3 more authors) (2014) Microstructure and durability of alkali-activated materials as key parameters for standardization. *Journal of Sustainable Cement-Based Materials*, 4 (2). pp. 116-128. ISSN 2165-0373

<https://doi.org/10.1080/21650373.2014.979265>

---

**Reuse**

Unless indicated otherwise, fulltext items are protected by copyright with all rights reserved. The copyright exception in section 29 of the Copyright, Designs and Patents Act 1988 allows the making of a single copy solely for the purpose of non-commercial research or private study within the limits of fair dealing. The publisher or other rights-holder may allow further reproduction and re-use of this version - refer to the White Rose Research Online record for this item. Where records identify the publisher as the copyright holder, users can verify any specific terms of use on the publisher's website.

**Takedown**

If you consider content in White Rose Research Online to be in breach of UK law, please notify us by emailing [eprints@whiterose.ac.uk](mailto:eprints@whiterose.ac.uk) including the URL of the record and the reason for the withdrawal request.



[eprints@whiterose.ac.uk](mailto:eprints@whiterose.ac.uk)  
<https://eprints.whiterose.ac.uk/>

# MICROSTRUCTURE AND DURABILITY OF ALKALI-ACTIVATED MATERIALS AS KEY PARAMETERS FOR STANDARDISATION

**Jannie S.J van Deventer**<sup>(1)(2)</sup>, **Rackel San Nicolas**<sup>(2)(3)(4)</sup>, **Idawati Ismail**<sup>(2)(5)</sup>, **Susan A. Bernal**<sup>(6)</sup>, **David G. Brice**<sup>(1)(2)</sup> and **John L. Provis**<sup>(6)</sup>

(1) Zeobond Pty Ltd, P.O. Box 23450, Docklands, Victoria 8012, Australia

(2) Geopolymer and Mineral Processing Group, Department of Chemical & Biomolecular Engineering, University of Melbourne, Victoria 3010, Australia

(3) Department of Infrastructure Engineering, University of Melbourne, Victoria 3010, Australia

(4) Centre of Sustainable Infrastructure, Faculty Science, Engineering and Technology, Swinburne University of Technology, PO Box 218, Hawthorn, Victoria 3122, Australia

(5) Faculty of Engineering, Universiti Malaysia Sarawak, Kota Samarahan 93400, Sarawak, Malaysia

(6) Department of Materials Science and Engineering, University of Sheffield, Sir Robert Hadfield Building, Mappin Street, Sheffield S1 3JD, United Kingdom

## **Abstract**

Alkali-activated concrete (AAC) has been commercialised as a low-CO<sub>2</sub> construction material, but its adoption still faces several challenges, including standardisation, lack of a dedicated supply chain, limited service track record, and the question of whether laboratory durability testing can predict service life. This paper outlines how using different precursors leads to the formation of different AAC phase assemblages, and how AAC can be recognised in standards using a performance-based approach independent of binder chemistry. Microstructural assessment of pastes, strength development, water permeability and chloride migration of two AACs (100% slag and 1:1 slag:fly ash) are presented, and compared to Portland cement concrete. Manipulation of binder chemistry leads to differences in the properties of the AACs; however, both AACs assessed exhibited technical benefits in a performance-based comparison. AACs can meet the requirements of the equivalent performance concept, independent of the binder chemistry, supporting their scale-up, regulatory acceptance and wider adoption.

**Keywords:** alkali-activated concrete, blast furnace slag, fly ash, microstructure, durability, commercialisation

## **1. INTRODUCTION**

Over the past decades, many formulations of cements have been investigated as lower-CO<sub>2</sub> alternative to ordinary Portland cement (OPC). The first generation of these ‘greener’ cements involved blends of OPC and supplementary cementitious materials (SCM), which are now used in structural concrete all over the world for performance as well as environmental reasons [1]. The second generation includes alkali-activated cement/ concrete (AAC) [2], which does not contain OPC and is currently being introduced into the market [3, 4]. As with all concretes, AAC must meet the mechanical strength and workability requirements of civil construction,

and be durable over an extended service life. A main hurdle currently preventing wide-spread implementation of AAC in construction is the lack of substantial long-term durability data proving the structural integrity of the material throughout its life-cycle [5, 6].

The conventional approach to determine durability of cementitious materials is to set up in-service test sites, which collect information on the concrete over a prolonged period of time, usually on the order of decades, for various aggressive environments. These data, in combination with laboratory testing, would enable various standards organisations (such as CEN and ASTM) to create prescriptive standards for AAC, as already exist for OPC and SCM blends. However, this approach is hardly feasible in view of the urgency to start using low CO<sub>2</sub> emissions cements such as AAC in modern construction.

There are several aspects to consider when assessing durability of non-Portland binders, such as the differences in chemistry and phase assemblage compared with OPC, and the real applicability of those tests to evaluate material performance under exposure to aggressive agents, taking into account that those protocols have been developed for OPC testing. Therefore, in evaluating the durability of AAC, it is essential to carry out validation and development of a deeper understanding of the existing testing standards, in order to generate reliable results that can be used for the prediction of long-term performance [6]. This is a critical aspect, as quantification of AAC durability relates to the prediction of service life, and this is one of the main challenges facing the commercial adoption of AAC.

Efforts are underway to change the standards culture from prescriptive-based to performance-based, in order to overcome the existing challenges in applicability of different testing protocols, especially for materials with different chemistries. This approach allows more rapid adoption of alternative binders in the construction industry, as it aims to achieve given performance levels, instead of following prescriptive rules of mix design proportioning. Performance-based standards will require that a particular AAC has equivalent engineering performance and durability in an environment when compared with a reference Portland cement concrete [7, 8].

Ground granulated blast furnace slag (GGBFS) and fly ash (FA) are currently accepted as attractive precursors for large-scale industrial production of AACs [9], as concretes based on these materials develop high mechanical strengths, and can have more favourable rheological properties and lower water demand, compared with mixes based on calcined clays [10]. AACs containing different ratios of GGBFS and FA have been extensively assessed, and used for large scale structural applications over the past decades. These materials are expected to provide a good synergy between mechanical strength and durability, making use of the stable coexistence of the hydration-reaction products characteristic of alkali-activated GGBFS (mainly C-S-H gels) and alkali-activated aluminosilicates (geopolymer gel). Also, blending aluminosilicate-rich materials, such as fly ash, within alkali-activated slag binders has facilitated the use of aluminosilicate wastes or by-products which may be insufficiently reactive to develop good mechanical strength when activated alone, providing a pathway to valorisation of such materials [11].

The optimal proportions of any two precursors in an AAC will depend on their relative reactivity, price, availability, the specific application, and technical requirements such as high early strength, specific workability, desired permeability, or mass transport resistance. In alkali-activated blended concretes these properties are strongly influenced by the content of fly ash incorporated [12]. Recent studies [13-16] have demonstrated that the durability of an AAC based on GGBFS/FA blends is directly linked to the microstructure of the reaction products forming in these binders, as a function of the nature and concentration of the activator, and also the maturity of the material. This is associated with the fact that the microstructure controls the transport properties of the binder and the stability of the matrix when exposed to aggressive agents.

Considering the number of variables controlling the properties of AAC, this paper presents a correlation between the microstructural features and a performance-based analysis of the durability of AACs, by comparing the strength development, water permeability and diffusional transport properties of 100% GGBFS and 50% GGBFS/50% FA-based AACs with a 100% OPC concrete. This work demonstrates that the durability of AAC is directly linked to the microstructure developed in these materials, and therefore, it is feasible to design AAC for a given service and required performance. A discussion of the importance of durability studies and the role of research in the commercialisation process of these materials is also presented.

## 2. MATERIALS AND METHODS

### 2.1. Materials

The Portland cement (OPC) used for the reference samples was type GP according to Australian Standard AS 3972-2010 [17] (Eureka Cement, Australia). GGBFS supplied by Zeobond Pty Ltd, Melbourne, and a Class F FA from Bayswater Power Station in New South Wales, Australia, were used as raw materials for AAC. The chemical composition and physical properties of these materials are presented in Tables 1 and 2, respectively.

Table 1: Composition of OPC, GBFS and FA from X-ray fluorescence analysis. LOI is loss on ignition at 1000°C

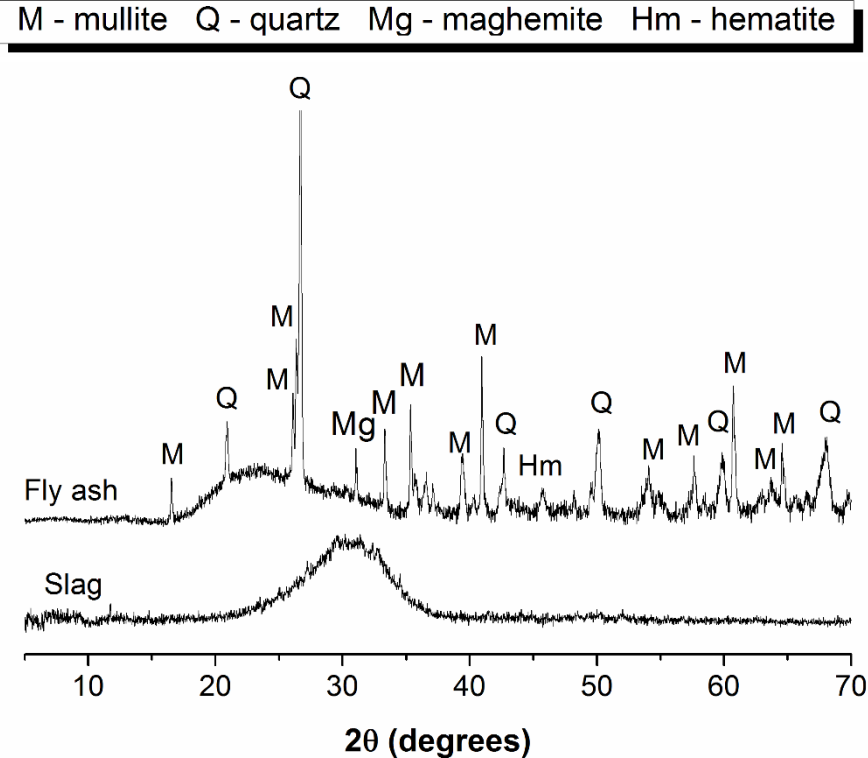
Oxides, wt %	SiO <sub>2</sub>	Al <sub>2</sub> O <sub>3</sub>	Fe <sub>2</sub> O <sub>3</sub>	CaO	MgO	SO <sub>3</sub>	Na <sub>2</sub> O	K <sub>2</sub> O	LOI
OPC	20.3	4.5	4.6	62.9	1.2	2.6	0.3	0.3	3.3
GGBFS	34.2	13.8	0.4	43.1	5.4	0.8	0.1	0.4	1.8
Fly ash	63.9	25.3	5.3	< 0.1	1.0	0.2	0.2	1.3	2.7

Table 2: Physical properties of the source materials

	Specific gravity (kg/m <sup>3</sup> )	Average particle size (d <sub>50</sub> ) (µm)*
OPC	3200	8
GGBFS	2800	15
Fly ash	2200	12

\* Determined by laser diffraction

The X-ray diffractograms of the anhydrous fly ash and slag are shown in Figure 1. The unreacted fly ash shows, as main crystalline phases, quartz ( $\text{SiO}_2$ , Powder Diffraction File (PDF) # 01-079-1910), mullite ( $\text{Al}_6\text{Si}_2\text{O}_{13}$ , PDF# 00-015-0776), hematite ( $\text{Fe}_2\text{O}_3$ , PDF# 00-033-0664), and maghemite ( $\text{Fe}_2\text{O}_3$ , PDF# 00-039-1346). Meanwhile the unreacted slag does not show reflection of any crystalline phases, indicating that this is a highly glassy material.



**Figure 1:** X-ray diffractograms of unreacted slag and unreacted fly ash

As coarse aggregate an alluvial siliceous aggregate of 20 mm maximum size with specific gravity of  $2830 \text{ kg/m}^3$  and water absorption of 1.10% was used. The fine aggregate was a silica sand with a specific gravity of  $2550 \text{ kg/m}^3$  and water absorption of 0.90%.

Paste and concrete samples produced using a blend of NaOH pellets, tap water, and a commercial silicate (PQ Grade D) solution, to achieve a molar ratio of  $\text{SiO}_2/\text{Na}_2\text{O}$  of 1.0, an activator dose of 8 g  $\text{Na}_2\text{SiO}_3$  per 100g of slag.

**2.2. Mix proportions**

**2.2.1. Paste**

Two alkali-activated binders were produced: one solely based on GGBFS, and a blended systems with 50 wt.% GGBFS/ 50 wt.% FA. These binders were mixed with an activator solution dose of 8 g  $\text{Na}_2\text{SiO}_3$  per 100 g of anhydrous GGBFS+FA. OPC paste was also produced for comparison purposes. Similar water/ binder (w/b) ratios to those specified for the concretes (Table 3) were adopted for preparing these pastes. The pastes were poured in 15 mL

centrifuge tubes and cured under sealed conditions at room temperature (20-23 °C) until testing. At 28 and 90 days of curing, the specimens were demoulded, crushed and immersed in acetone for 30 min. Afterwards the samples were filtered and kept in a desiccator for 24h to remove the remnant solvent prior to analysis.

### 2.2.2. Concretes

Concretes were mixed in an electric pan mixer following Australian Standard AS 1012.2 [18], according to the formulations in Table 3. AAC were produced using similar proportions of FA and GBFS as the main binder components, with water to binder ratios (w/b) selected to meet targeted strengths of  $50 \pm 3$  MPa after 28 days of curing.

Table 3: Formulation of the concretes

Sample ID	OPC (kg/m <sup>3</sup> )	GGBFS (kg/m <sup>3</sup> )	FA	w/b	Aggregates (kg/m <sup>3</sup> )		Activator concentration (wt.%)	Slump (mm)
					Coarse aggregate	Fine aggregate		
100OPC	360	-	-	0.52	1150	720	-	90
AA100S	-	400	-	0.44	1150	640	8	130
AA50S/50FA	-	200	200	0.36	1150	640	8	110

Each batch comprised around 40 L of concrete, which was cast in 100 mm diameter × 200 mm height cylinder moulds for mechanical and durability tests. In fresh state concretes, workability was measured accordingly with the ASTM C143M-05 [19]. It has been object of extensive discussions whether this is a suitable method to study the rheological behaviour of alkali-activated concretes or not; however, we decided to follow this methodology, as this test is carry out by concrete practitioners, and the results can be directly compared with those of Portland cement based concretes.

After 24 h of sealed curing at 99% relative humidity and room temperature (21 °C), specimens were cured at ambient temperature (20-23 °C) under water until the testing age.

## 2.3. Experimental procedures

### 2.3.1. Characterisation of the paste

Microstructural analysis of the binders after 28 and 90 days of curing was carried out via X-ray diffraction (XRD) using a Bruker D8 Advance instrument, scanning from 5° - 65° 2 $\theta$ , with a 0.02° step size and 2 s/step count time. Environmental scanning electron microscopy (ESEM) was conducted using an FEI Quanta instrument with a 15 kV accelerating voltage and a working distance of 10 mm. Polished samples were evaluated in low vacuum mode, using a backscatter detector to avoid the need for carbon coating of the samples. A Link-Isis (Oxford Instruments) energy dispersive X-ray (EDX) detector was used to determine chemical compositions.

### 2.3.2. Characterisation of the concretes

Compressive strength tests were carried out after 1, 7, 28, 56, and 90 days on 100 mm diameter  $\times$  200 mm height specimens following ASTM C39-10 [20], using an ELE ADR Auto 1500 instrument. Specimens were loaded at a rate of 2.4 kN/sec until failure.

The ASTM C642-06 [21] protocol was used to determine the volume of permeable voids (VPV). Before the test, the samples were pre-conditioned by drying at 100 °C until reaching constant weight, i.e. a difference in weight of less than 0.5% between two consecutive measurements. It is worth noting that the pre-conditioning used is severe, and in the case of alkali-activated materials, it has been demonstrated that such treatment can induce microstructural changes and microcracking [22]. However, the standardised method has been adopted in this study to facilitate the direct comparison of Portland and alkali-activated concretes. Chloride transport was assessed according to the non-steady state migration test, NT Build 492 [23]. All durability-related characteristics reported here correspond to an average of 4 measurements on different samples, cured for 28 and 90 days.

## 3. RESULTS AND DISCUSSION

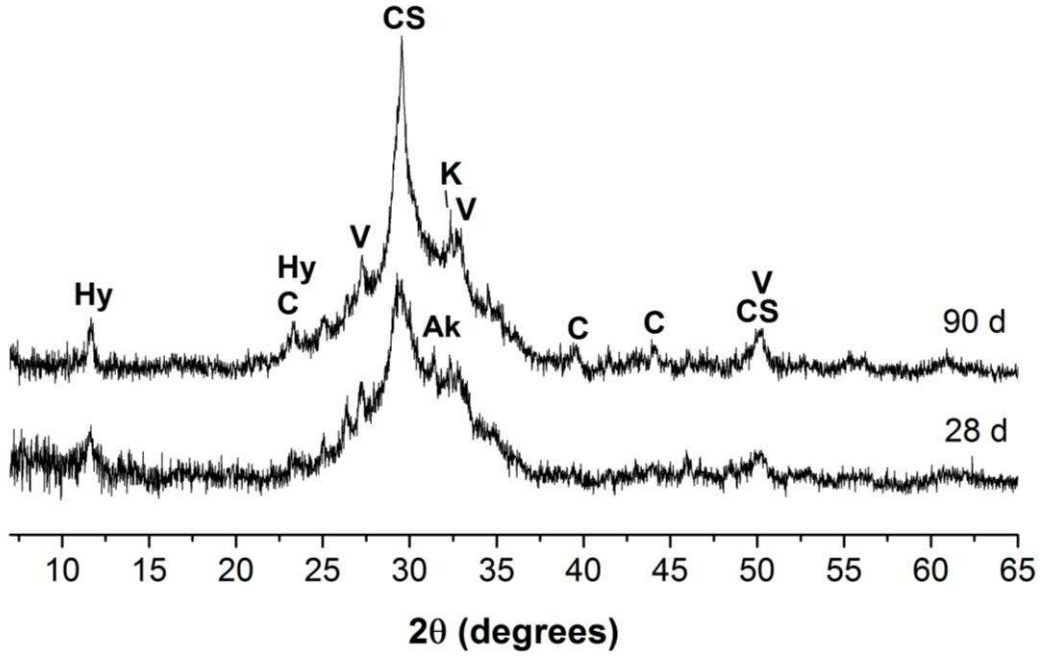
### 3.1. Microstructural characterisation of the binders

#### 3.1.1. X-ray diffraction

In AA100S pastes (Figure 2A) a calcium silicate hydrate (C-S-H) with a riversideite-9Å type structure ( $\text{Ca}_5\text{Si}_6\text{O}_{17}\cdot\text{H}_2\text{O}$ ; Powder Diffraction File (PDF) # 029-0329) is observed. The main reflection assigned to this phase ( $29.5^\circ 2\theta$ ) sharpens and becomes more intense as reaction progresses. Formation of the layered double hydroxide hydrotalcite ( $\text{Mg}_6\text{Al}_2\text{CO}_3(\text{OH})_{16}\cdot 4\text{H}_2\text{O}$ ; PDF# 014-0191), along with traces of the calcium carbonates calcite (PDF# 01-083-0577), and vaterite (PDF# 01-074-1867) (all polymorphs of  $\text{CaCO}_3$ ) are observed. Hydrotalcite is one of the main reaction products in alkali-activated slag pastes when Mg is present, independent of the activator used [24-26]. Carbonate formation in these samples is associated with superficial weathering of the samples during handling, crushing and/or analysis. Traces of katoite (siliceous hydrogarnet,  $\text{Ca}_3\text{Al}_2(\text{SiO}_4)_{3-x}(\text{OH})_{4x}$  with  $1.5 \leq x \leq 3.0$ , PDF# 038-0368) were also detected after 90 days of curing.

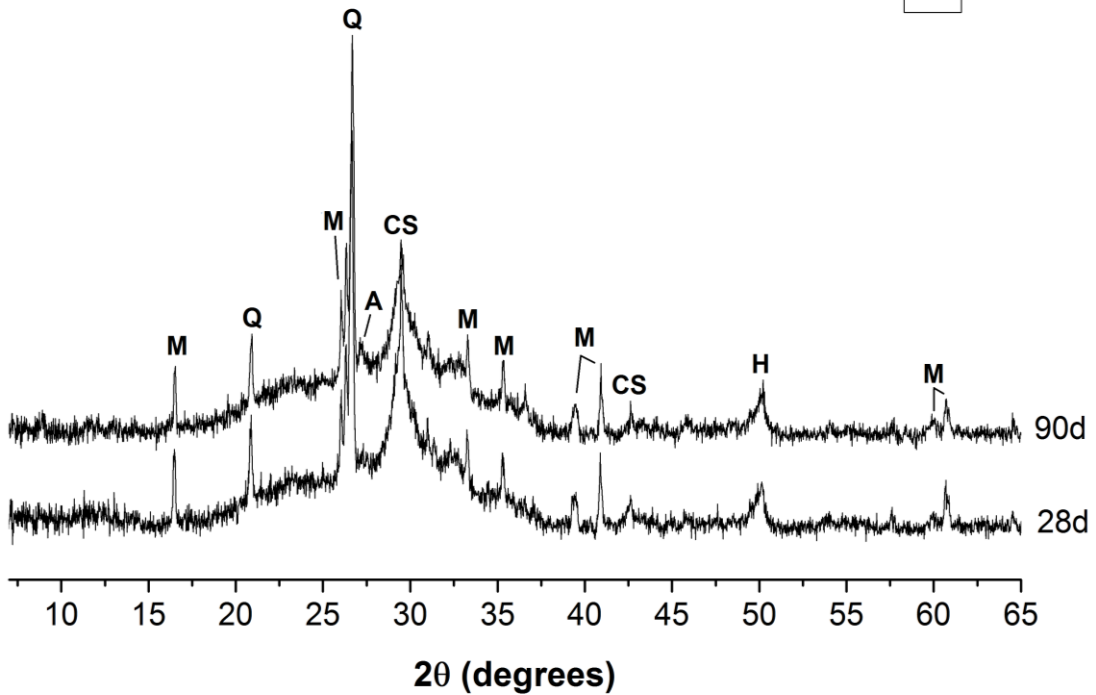
Hy - hydrotalcite CS - calcium silicate hydrate  
V - vaterite C - calcite Ak - akermanite K - katoite

**A**



M - mullite Q - quartz H - hematite A - aragonite  
CS - calcium silicate hydrate

**B**



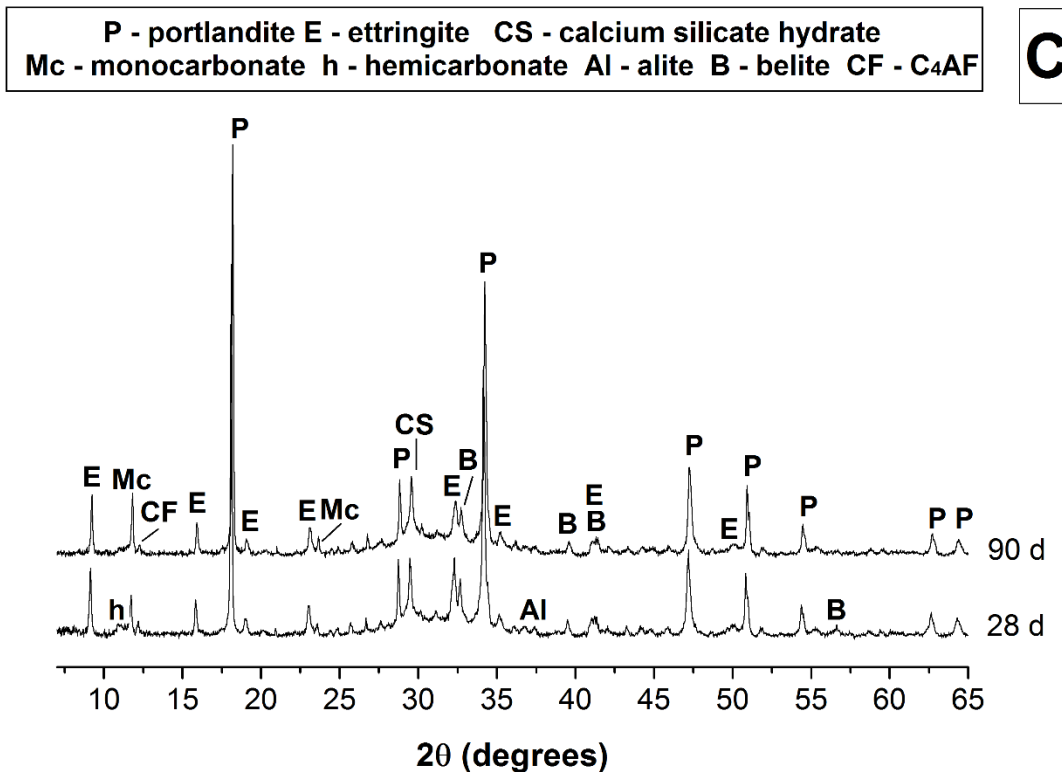


**Figure 2:** X-ray diffractograms of AAC based on (A) 100% slag, (B) 50% slag / 50% fly ash, and (C) OPC pastes, as function of the time of curing

In the AA50S/50FA paste (Figure 2B) a C-S-H type phase is identified as main crystalline reaction products: a tobermorite 11Å ( $\text{Ca}_5(\text{OH})_2\text{Si}_6\text{O}_{16} \cdot 4\text{H}_2\text{O}$ ; PDF #00-019-1364). Hydrotalcite was not identified as a reaction product in this mix. Traces of the calcium carbonate polymorph aragonite were also observed, associated with the weathering of the samples. Reflections of hematite ( $\text{Fe}_2\text{O}_3$ ; PDF# 00-001-1053), mullite ( $\text{Al}_6\text{Si}_2\text{O}_{13}$ ; PDF# 00-015-0776) and quartz ( $\text{SiO}_2$ ; PDF# 00-033-1161) are also identified. These phases are present in the unreacted fly ash, and it has been identified that they do not participate in the alkali-activation reaction [12, 14].

In the hydrated OPC sample (Figure 2C), traces of the Portland clinker phases alite ( $\text{Ca}_3\text{SiO}_5$ ; PDF # 04-009-5560), tetracalcium aluminoferrite ( $\text{C}_4\text{AF}$ ) and belite ( $\text{Ca}_2\text{SiO}_4$ ; PDF # 01-083-0460) are present, along with minor quartz and vaterite. The dominant binder phase is a disordered C-S-H phase. As crystalline hydration products portlandite ( $\text{Ca}(\text{OH})_2$ ; PDF# 00-044-1481) and ettringite ( $\text{Ca}_6\text{Al}_2(\text{SO}_4)_3(\text{OH})_{12} \cdot 25\text{H}_2\text{O}$ ; PDF # 00-009-0414) were identified; traces of AFm phases, most likely calcium (mono,hemi)carboaluminate, are also identified, although these phases appear disordered. The reflections of all phases in this sample were assigned considering the results reported by Lothenbach et al. [27].

These results show the significant differences in the phase assemblage of alkali-activated slag binders when blended with an aluminosilicate precursor, such as fly ash. Likewise, it is clearly

identified that the nature of reaction products forming in alkali-activated materials and hydrated Portland cement is completely different, and therefore realistic direct comparison of these materials cannot be carried out without considering these chemical differences, unless a performance-based approach is adopted. A detailed discussion of the differences in the crystalline products forming in these types of binders is reported in [28].

### 3.1.2. Scanning electron microscopy

Even though the nature of the reaction products forming in AAC and OPC differs, the formation of C-S-H type phases is identified in both of these systems. It is well known that this is the main strength giving phase in both binder types, and therefore a detailed understanding of any differences in the C-S-H forming in OPC and under highly alkaline conditions (such as those reached in AAC) is required. Figure 3 summarises the results of EDX analysis of the main binder phases of AA100S, AA50S/50FA and OPC, where the analysis was conducted specifically on binder regions excluding remnant precursor particles wherever possible. It is clearly identified that the C-S-H forming in OPC has a higher Ca and lower Al content than the C-A-S-H forming in AA100S. In AA50S/50FA, significant variability in the composition of the C-A-S-H phase is observed. In this system the formation of two distinct phases is taking place: there are high and low Ca type phases with varying Al/Si ratio. Both reaction products show Al/Si ratios within the ranges identified for N-A-S-H type phases typically forming in alkali-activated fly ash [16, 29]. These results suggest that the activation of both GGBFS and FA is occurring under the activation conditions used in this study; however the presence of Ca in the system seems to inhibit the formation of pure N-A-S-H type gel. Similar results have been identified by García-Lodeiro et al. [29-31], who identified formation of a N-(C)-A-S-H phase when assessing the compatibility of these binding gels, independent of the Ca content in the system. The microstructures of each of these phases are expected to be different, as their chemical composition varies, and the stability at high temperatures and under exposure to aggressive agents. So, the formation of any type of hybrid binding phases is likely to have significant implications in the performance of alkali-activated blended systems including both a Ca source and an aluminosilicate precursor.

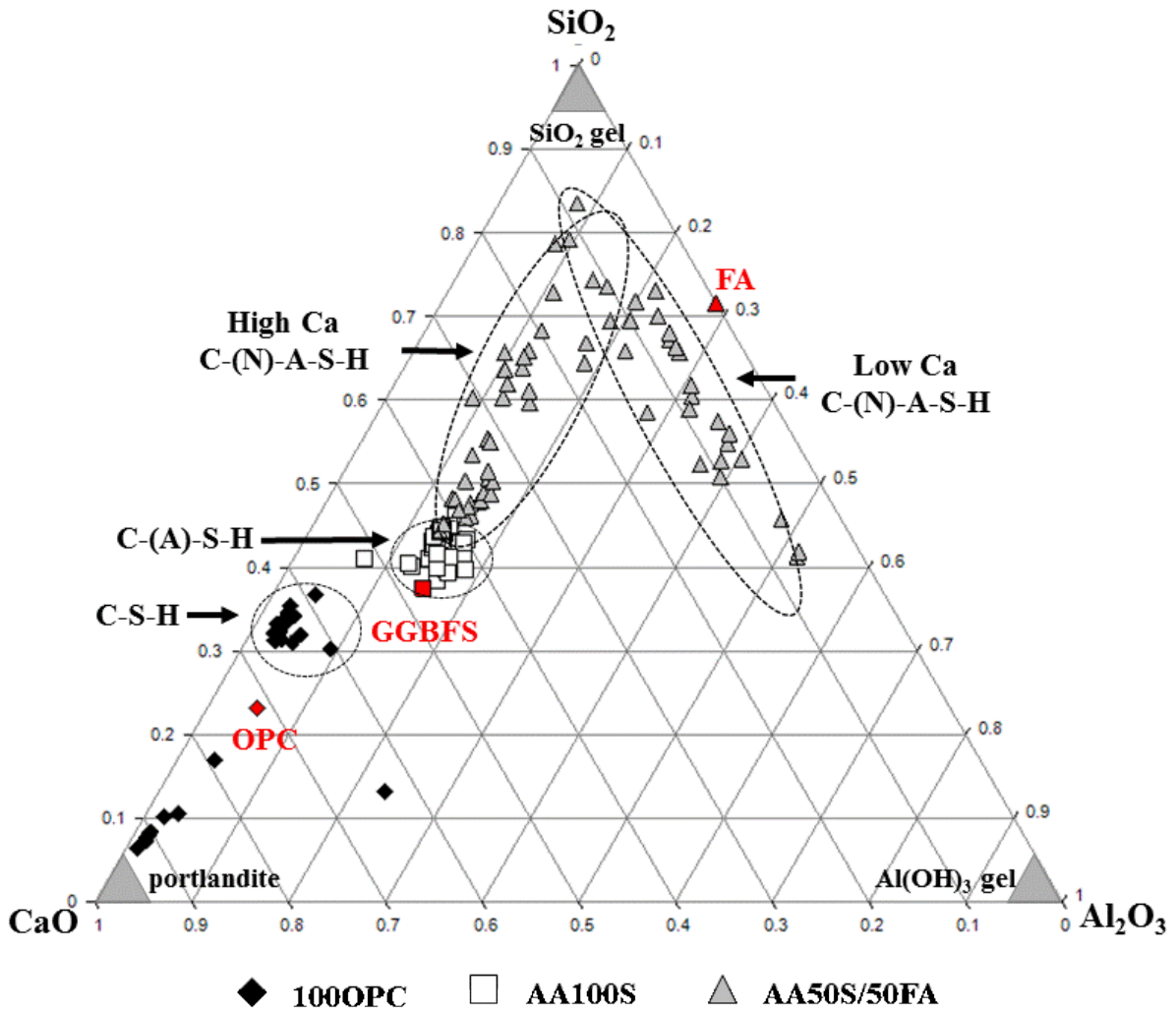


**Figure 3:** Pseudo-ternary plot of binder gel compositions measured by SEM-EDX after 28 days of curing of OPC, and AAC pastes

### 3.2. Performance of the concretes

#### 3.2.1. Compressive strength

Table 4 presents the compressive strengths of the concrete specimens as a function of the time of curing. Both AACs and the reference OPC concrete all satisfied the strength target of  $55 \pm 4$  MPa after 28 days of curing.

Table 4: Compressive strengths of AAC and OPC concretes as function of the time of curing. Each result is the mean of 4 specimens tested, standard deviations are all <10%.

Time of curing	Compressive strength (MPa)		
	100OPC	AA100S	AA50S50FA
1 day	11.9	19.9	10.7
7 days	38.8	46.8	48.5
14 days	42.9	48.4	53.8
28 days	51.6	58.1	57.8
56 days	57.9	61.0	59.8
90 days	61.4	65.7	63.1

These results suggest differences in the reaction rates between the two AACs and the OPC concrete. After 1 day of curing, the compressive strength of AA100S reaches a higher strength than the reference OPC. The substitution of 50% of GGBFS by FA in the AAC matrix affects the one day strength, which can be explained by the slower reactivity of FA than GGBFS. After 7 days of curing both AACs show higher strength than the OPC reference, and after 7 days the AA50S50FA has caught up its earlier delay. From 7 to 90 days the difference between the AAC and OPC is reduced, as the OPC concrete formulated at a relatively high water/cement ratio continues to hydrate.

### 3.2.2. Water absorption properties

Figure 4 shows the difference in water absorption as measured by the ASTM C642 boiling test for each mix design from 7 to 90 days of curing. After 7 or 28 days of curing the water absorption measurements are similar for all concretes. After 28 days of curing the measured volume of permeable voids (VPV) values of all concretes seem to increase, which is not an expected trend as the concrete is supposed to densify over time [32]. At 56 days of curing the AAC seems to have a higher VPV than the OPC. It is noteworthy that the VPV of the AA100S is constantly higher than the OPC and the AA50S/50FA, especially after 90 days. It has been shown that the C-A-S-H type gel forming in GGBFS-based AAC undergoes severe desiccation that can lead to micro-cracking when subjected to harsh drying conditions, such as those required by the ASTM C642 test [15, 22]. This explains these higher VPV values. Considering this, it could be assumed that the VPV increased over the time of curing in these samples because a larger fraction of C-A-S-H is forming as the reaction progresses, which can then be dehydrated during the pre-conditioning required to determine the VPV.

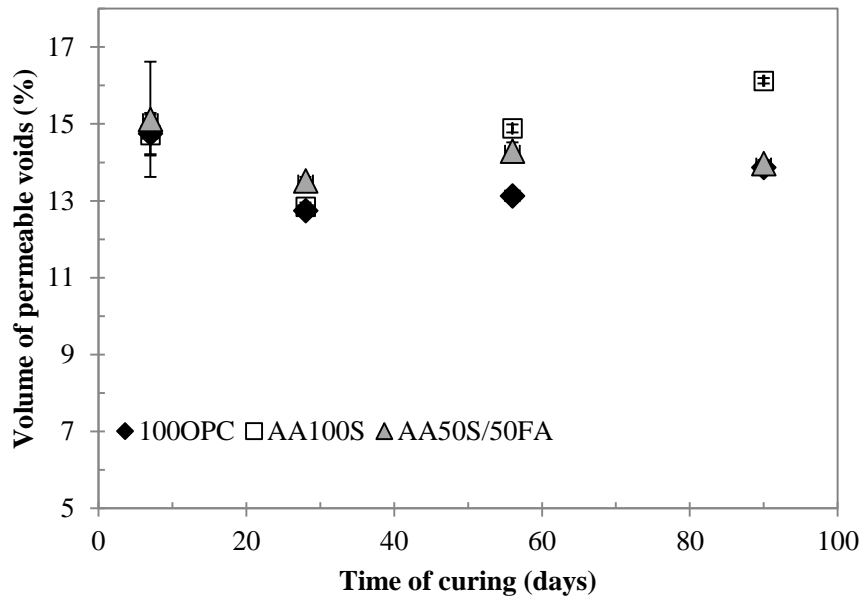


**Figure 4:** Volume of permeable voids of AAC and OPC concretes as function of the time of curing

The lower VPV values of the blended AA50S/50FA binder, which are comparable to the OPC, indicate that the addition of FA changes the nature of the gel and hence the stability of the binding phases. As identified by SEM-EDX (Figure 3), the inclusion of FA in the AA100S favours the formation of two distinctive C-(N)-A-S-H phases, with varying Ca and Al content, making evident that the coexistence of distinct C-A-S-H and N-A-S-H is not occurring in alkali-activated GGBFS/FA binders, but rather that these phases are highly intermixed. It has been identified [22] that limited variations in the structure of the C-(N)-A-S-H product forming in AA50S/50FA take place upon exposure to severe drying conditions. This elucidates that it is likely that the concretes produced with these binders undergo negligible changes during specimen pre-conditioning, and therefore reporting lower VPV values than obtained in AA100S and OPC, which are mainly composed of C-S-H and C-A-S-H phases. The role of Al and Ca in the C-A-S-H phase, and especially its higher potential to undergo desiccation, is an active area of research that needs further investigation, as it controls the durability of AAC and blended Portland systems.

Figure 5 depicts the VPV at 28 days plotted as a function of the compressive strength for each concrete. According to the classification of the durability guide AFGC AFREM 2004 [33], the AACs formulated here are in the same durability class as the OPC concrete. A slight increase in porosity can be distinguished, but this is minor considering the variability of the results, while retaining the same durability class. It remains questionable whether this type of VPV testing is reflective of in-service durability despite its importance to certain specifiers in Australia, as it has been proven [22] that the specified pre-conditioning of the specimens required by this test changes the microstructure of AAC, and therefore may provide misleading results. The

identification and validation of alternative protocols to determine porosity of these materials, minimising impacts on their in-service microstructure, is urgently required.

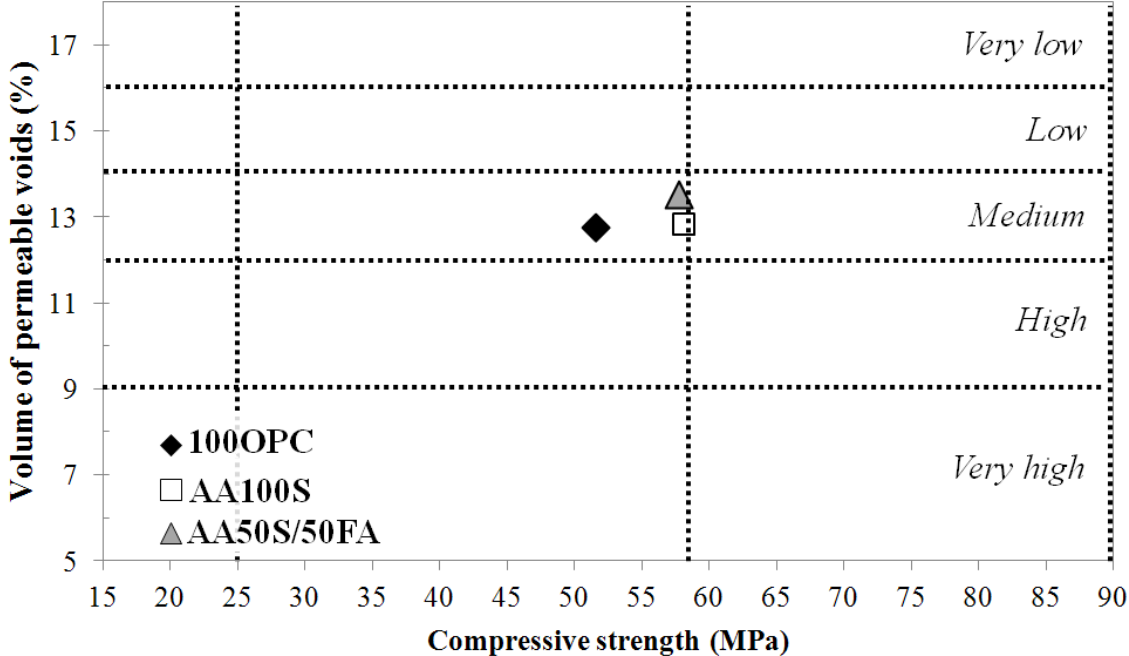


**Figure 5:** VPV as a function of compressive strength at 28 days for 100OPC, AA100S and AA50S50FA, and durability classes according to Baroghel-Bouny [32].

3.2.2 Chloride migration

Figure 6 shows that for each concrete, the higher the compressive strength, the lower the chloride diffusion coefficient as measured by the NordTest NT Build 492 method. For an equal strength class, AAC has a lower chloride diffusion coefficient than the OPC after 28 or 90 days of curing. According to the classification of the durability guide [33], AAC will have better durability in seawater. The very low chloride diffusion coefficient of AAC, especially that of AA100S at 90 days, contrasts with the higher VPV value of the slag-only AAC. This indicates that there is not a direct correlation between ASTM C642 VPV measurements and the actual rate of migration of aggressive agents in these concretes, and demonstrates the complexity of durability tests and the challenge of service-life prediction for a new construction material.

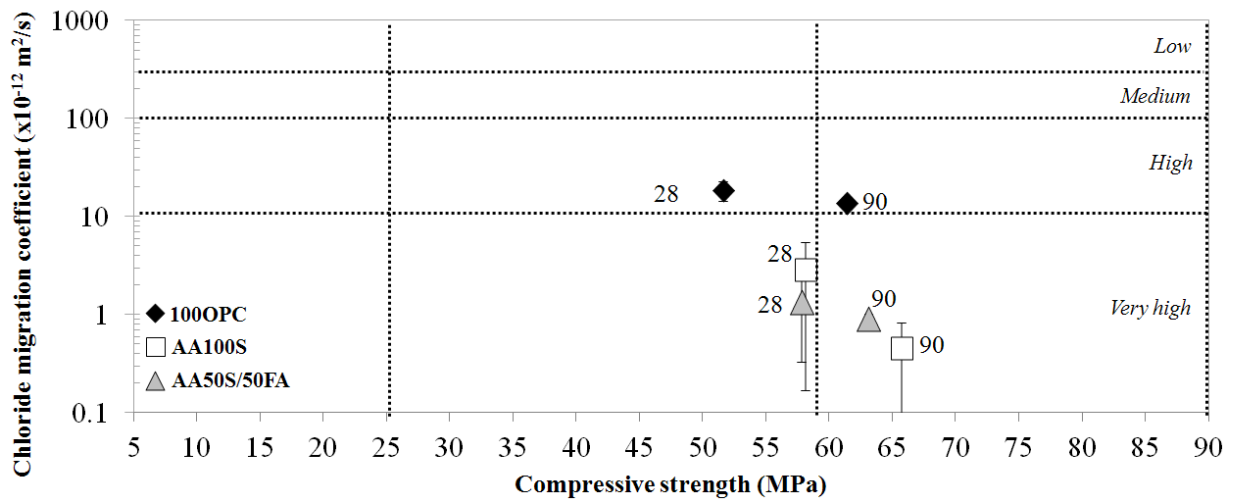


**Figure 6:** Chloride migration coefficient versus compressive strength at 28 and 90 days for 100OPC, AA100S and AA50S50FA, and durability classes according to [32].

#### 4. PATHWAYS TO COMMERCIALISATION AND THE ROLE OF RESEARCH

Although it has been demonstrated that AAC production involves significant reduction in CO<sub>2</sub> emissions [34], industry confidence in AAC needs to be built gradually from both a technical and commercial standpoint. There are only a few examples of AAC in long term structural applications (more than 50 years use) that can demonstrate the long service life of this emerging construction material [4]. The past 40 years have seen significant research in OPC concrete that has led to cost reduction and new engineering applications, and consequently OPC concrete formulation is now well established and has application specific prescriptions. Being a new technology, AAC durability needs to be carefully assessed and understood in order to develop industry and consumer confidence [5, 6].

The development of a deep understanding of the chemical and physical processes governing AAC durability is essential if practitioners are to ensure that alternative materials can meet the requirements of designated applications. The strength of a construction material often receives the most attention from specifiers, however it is not the only important criterion when selecting a material. The results presented in section 3.2.1 show that AAC mixes can meet a required strength development profiles when formulated appropriately, starting from precursors with very different reactivities. The durability of AAC depends on numerous parameters, including the nature of the raw materials, curing conditions and mix design, hence assessment of AAC durability is an immense task. It is essential to involve parties including consulting engineers, key specifiers, standards committee members, asset owners, government officials and construction companies in this task, as buy-in from these parties is as important as technical development [35].

Although there is formal recognition of AAC as being equivalent to OPC by a state roads authority, VicRoads, in Australia [36, 37], AAC is not in general accepted in concrete standards worldwide. The lack of a long in-service track record for AAC necessitates a performance-

based approach linking diffusional transport properties to durability, valid for any concrete independent of its chemistry or phase composition. One approach is to utilise empirical data collected in aged OPC concretes (~100 years), and based on that information develop durability classes [33], defined in terms of service life, to predict the service life of AAC. A normative comparison of diffusional transport properties of AAC and OPC concretes as a predictor of service life could provide a basis for making the case for the durability of AAC without waiting many decades. However, not all durability tests currently accepted for OPC concrete are valid and suitable for AAC, particularly highly accelerated tests, as these can be strongly influenced by binder chemistry and microstructure [6].

Confidence in AAC has to be built step by step by gradually tackling more advanced applications, especially regarding durability, as has been done previously for OPC and OPC+SCM blended concretes [37]. Each application requires knowledge of the specific characteristics of the material to meet set targets, and so close collaboration between academic researchers and industry is helpful in adapting AAC mix designs to a specific situation. In practice, several possible formulations of AAC are first tested in the laboratory or at pilot-scale. A formulation will then be chosen by the research team according to the availability of the precursors and the specific performance target. Subsequently, multiple production trials are typically conducted using manufacturing-scale equipment. Finally, standard, independent and accredited OPC-based performance tests are used to ensure that the product meets basic specifications for the application targeted. Gradually, knowledge of the product is gained and enriched by continuous feedback from both on-site data and research [37].

Experience shows that to build confidence in AAC, small ‘low risk’ projects have to be successfully executed; most customers and end users are more readily open to initially undertake projects of lowest risk, such as footpaths, kerb and channel, and low-strength pits, as the cost of replacement is low in case performance requirements are not met. As technical risk increases for an application, testing requirements and the demonstration of technical capability increase. This is particularly so in Australia, the USA or Europe because of the entrenched standards, but may not be the case in developing countries, which are generally more willing to accept an innovative solution to a problem such as cement replacement when market demand exceeds supply; this may present an opportunity to commercialise AAC more rapidly. Markets where waste generation rather than CO<sub>2</sub> emission is likely to become increasingly a political issue, particularly China and India where fly ash is available due to the wide use of coal power generation, may prove to be the primary areas in which AAC becomes accepted on a regulatory level.

As with the commercialisation of all new technologies, even with pressure to select a more ‘environmentally friendly’ cement, the cost of the material will dictate the customer’s decision. The price is always location-specific and determined by many parameters including the availability of source materials and activators, logistical infrastructure, supply chain control, transport costs and volume of demand. The worldwide availability of reactive aluminosilicate materials (slag, fly ash, natural pozzolans, among others) and bulk alkali activators alone does not guarantee AAC to be price-competitive when compared to OPC. Instead, the capacity of an AAC producer to control the processing and supply of such materials in bulk is more important

to ensure price-competitiveness. This remains a challenge while production volumes of AAC are small and recognition in standards is lacking.

## 5. CONCLUSIONS

International efforts are underway to change the standards culture from prescriptive-based to performance-based, which will facilitate a more rapid adoption of alternative cements by the construction industry. Despite this shift, there are still concerns about the durability of AAC and the relationship between accelerated testing and in-service performance. This paper shows that different testing methods could give different trends in predicted durability for AAC, which provides an obstacle to commercial adoption, as different concrete consultants favour different methods. It has been shown here that AAC concrete can have a slightly higher water permeability value than OPC concrete even when it is equivalent in durability. Migration of chloride ions is reduced in AAC as a result of the different gel chemistry, pore structure and transport properties of the concrete compared to OPC. In parallel with ongoing demonstration of AAC technology in large-scale projects and collaborative work with engineering consultants to build confidence, further research remains essential to link microstructure and phase evolution to durability testing and in-service performance of AAC. Of equal importance is the development of a price-competitive supply chain for AAC materials while recognition in standards is still lacking.

## ACKNOWLEDGEMENTS

Funding support is acknowledged from Zeobond Research Pty Ltd, from the Australian Research Council as part of grant LP0991550, and as PhD scholarship awarded to I. Ismail by the Ministry of Higher Education of Malaysia.

## REFERENCES

1. Lothenbach, B., K. Scrivener, and R.D. Hooton, Supplementary cementitious materials. *Cement and Concrete Research*, 2011. **41**(3): p. 217-229.
2. Duxson, P., et al., The role of inorganic polymer technology in the development of 'Green concrete'. *Cement and Concrete Research*, 2007. **37**(12): p. 1590-1597.
3. Provis, J.L., et al., Historical aspects and overview, in *Alkali-Activated Materials: State-of-the-Art Report*, RILEM TC 224-AAM, J.L. Provis and J.S.J. van Deventer, Editors. 2014, Springer/RILEM: Dordrecht. p. 11-57.
4. Provis, J.L., et al., Demonstration projects and applications in building and civil infrastructure, in *Alkali-Activated Materials: State-of-the-Art Report*, RILEM TC 224-AAM, J.L. Provis and J.S.J. van Deventer, Editors. 2014, Springer/RILEM: Dordrecht. p. 309-338.
5. Bernal, S.A., et al., Durability and testing - Degradation via mass transport, in *Alkali-Activated Materials: State-of-the-Art Report*, RILEM TC 224-AAM, J.L. Provis and J.S.J. van Deventer, Editors. 2014, Springer/RILEM: Dordrecht. p. 223-276.
6. Bernal, S.A. and J.L. Provis, Durability of alkali-activated materials: progress and perspectives. *Journal of the American Ceramic Society*, 2014. **97**(4): p. 997-1008.
7. Bickley, J., R. Hooton, and K. Hover, *Guide to Specifying Concrete Performance*. RMC Research & Education Foundation, 2008.

8. European Committee for Standardization (CEN), Concrete – Part 1: Specification, Performance, Production and Conformity (EN 206-1). 2010: Brussels, Belgium.
9. Duxson, P. and J.L. Provis, Designing precursors for geopolymer cements. *Journal of the American Ceramic Society*, 2008. **91**(12): p. 3864-3869.
10. Provis, J.L. and S.A. Bernal, Geopolymers and related alkali-activated materials. *Annual Review of Materials Research*, 2014. **44**: p. in press, DOI 10.1146/annurev-matsci-070813-113515.
11. Provis, J.L. and S.A. Bernal, Binder chemistry – Blended systems and intermediate Ca content, in *Alkali-Activated Materials: State-of-the-Art Report*, RILEM TC 224-AAM, J.L. Provis and J.S.J. van Deventer, Editors. 2014, Springer/RILEM: Dordrecht. p. 125-144.
12. Ismail, I., et al., Modification of phase evolution in alkali-activated blast furnace slag by the incorporation of fly ash. *Cement and Concrete Composites*, 2014. **45**: p. 125-135.
13. Bernal, S.A., et al., MgO content of slag controls phase evolution and structural changes induced by accelerated carbonation in alkali-activated binders. *Cement and Concrete Research*, 2014. **57**: p. 33-43.
14. Bernal, S.A., et al., Gel nanostructure in alkali-activated binders based on slag and fly ash, and effects of accelerated carbonation. *Cement and Concrete Research*, 2013. **53**: p. 127-144.
15. Ismail, I., et al., Influence of fly ash on the water and chloride permeability of alkali-activated slag mortars and concretes. *Construction and Building Materials*, 2013. **48**: p. 1187-1201.
16. Ismail, I., et al., Microstructural changes in alkali activated fly ash/slag geopolymers with sulfate exposure. *Materials and Structures*, 2013. **46**(3): p. 361-373.
17. Standards Australia, *General Purpose and Blended Cements (AS 3972-2010)*. 2010: Sydney.
18. Standards Australia, *Methods of testing concrete - Preparation of concrete mixes in the laboratory (AS 1012.2)*. 1993: Sydney, Australia.
19. ASTM International, *Standard Test Method for Flow of Hydraulic Cement Mortar (ASTM C1437 - 07)*. 2007: West Conshohocken.
20. ASTM International, *Standard Test Method for Compressive Strength of Cylindrical Concrete Specimens (ASTM C39/C39M - 10)*. 2010: West Conshohocken.
21. ASTM International, *Standard Test Method for Density, Absorption, and Voids in Hardened Concrete (ASTM C642 - 06)*. 2006: West Conshohocken, PA.
22. Ismail, I., et al., Drying-induced changes in the structure of alkali-activated pastes. *Journal of Materials Science*, 2013. **48**: p. 3566-3577.
23. Nordtest, *Concrete, mortar and cement-based repair materials: Chloride migration coefficient from non-steady state migration experiments (NT BUILD 492)*. 1999: Espoo, Finland.
24. Ben Haha, M., et al., Influence of activator type on hydration kinetics, hydrate assemblage and microstructural development of alkali activated blast-furnace slags. *Cement and Concrete Research*, 2011. **41**(3): p. 301-310.
25. Escalante-Garcia, J., et al., Hydration products and reactivity of blast-furnace slag activated by various alkalis. *Journal of the American Ceramic Society*, 2003. **86**(12): p. 2148-2153.
26. Fernández-Jiménez, A., et al., Structure of calcium silicate hydrates formed in alkaline-activated slag: Influence of the type of alkaline activator. *Journal of the American Ceramic Society*, 2003. **86**(8): p. 1389-1394.
27. Lothenbach, B., et al., Influence of limestone on the hydration of Portland cements. *Cement and Concrete Research*, 2008. **38**(6): p. 848-860.
28. Lecomte, I., et al., (Micro)-structural comparison between geopolymers, alkali-activated slag cement and Portland cement. *Journal of the European Ceramic Society*, 2006. **26**: p. 3789-3797.
29. García-Lodeiro, I., et al., Compatibility studies between N-A-S-H and C-A-S-H gels. Study in the ternary diagram Na<sub>2</sub>O-CaO-Al<sub>2</sub>O<sub>3</sub>-SiO<sub>2</sub>-H<sub>2</sub>O. *Cement and Concrete Research*, 2011. **41**(9): p. 923-931.

30. García-Lodeiro, I., Compatibility of cement gels C-S-H and N-A-S-H. Studies in real samples and in synthetic gels. 2008, Universidad Autónoma de Madrid: Madrid, Spain.
31. García-Lodeiro, I., et al., FTIR study of the sol-gel synthesis of cementitious gels: C-S-H and N-A-S-H. *Journal of Sol-Gel Science and Technology*, 2008. **45**(1): p. 63-72.
32. Hewlett, P.C., *Lea's Chemistry of Cement and Concrete*, 4th Ed. 1998, Oxford, UK: Elsevier. 1057.
33. Baroghel-Bouny, V., *Conception des bétons pour une durée de vie donnée des ouvrages, Maîtrise de la durabilité vis-à-vis de la corrosion des armatures et de l'alcali réaction, Etat de l'art et Guide pour la mise en œuvre d'une approche performantielle et prédictive sur la base d'indicateurs de durabilité*. 2004.
34. McLellan, B.C., et al., Costs and carbon emissions for Geopolymer pastes in comparison to Ordinary Portland Cement. *Journal of Cleaner Production*, 2011. **19**(9-10): p. 1080-1090.
35. Brice, D.G., et al., Conclusions and the future of alkali activation technology, in *Alkali-Activated Materials: State-of-the-Art Report*, RILEM TC 224-AAM, J.L. Provis and J.S.J. van Deventer, Editors. 2014, Springer/RILEM: Dordrecht. p. 381-388.
36. van Deventer, J.S.J., J.L. Provis, and P. Duxson, Technical and commercial progress in the adoption of geopolymer cement. *Minerals Engineering*, 2012. **29**: p. 89-104.
37. Van Deventer, J.S.J., et al. ST 1566: Development, standardization and applications of alkali-activated concretes. in *ASTM Symposium on Geopolymer Binder Systems*. 2013. San Diego, California: ASTM International.